Accurate Benchmark Calculation of the Reaction Barrier Height for Hydrogen Abstraction by the Hydroperoxyl Radical from Methane. Implications for C_nH_{2n+2} where $n = 2 \rightarrow 4$

Jorge Aguilera-Iparraguirre,*,† Henry J. Curran,‡ Wim Klopper,† and John M. Simmie‡

Institut für Physikalische Chemie, Universität Karlsruhe (TH), Karlsruhe, Germany, and Combustion Chemistry Centre, National University of Ireland, Galway, Ireland

Received: February 12, 2008; Revised Manuscript Received: May 13, 2008

The $CH_4 + HO_2^{\bullet}$ reaction is studied by using explicitly correlated coupled-cluster theory with singles and doubles (CCSD-R12) in a large 19s14p8d6f4g3h basis (9s6p4d3f for H) to approach the basis-set limit at the coupled-cluster singles−doubles level. A correction for connected triple excitations is obtained from the conventional CCSD(T) coupled-cluster approach in the correlation-consistent quintuple-ζ basis (cc-pV5Z). The highly accurate results for the methane reaction are used to calibrate the calculations of the hydroperoxyl-radical hydrogen abstraction from other alkanes. For the alkanes C_nH_{2n+2} with $n = 2 \rightarrow 4$, the reactions are investigated at the CCSD(T) level in the correlation-consistent triple-ζ (cc-pVTZ) basis. The results are adjusted to the benchmark methane reaction and compared with those from other approaches that are commonly used in the field such as CBS-QB3, CBS-APNO, and density functional theory. Rate constants are computed in the framework of transition state theory, and the results are compared with previous values available.

1. Introduction

In the detailed chemical kinetic modeling of hydrocarbon[1] and oxygenated fuels, hydrogen atom abstraction by the hydroperoxyl radical, $HO_2^{\bullet}$, is an important reaction class in the autoignition of fuels, particularly at low-to-intermediate temperatures in the range 600−1300 K. At these temperatures, most of the hydroperoxyl radicals are generated either by abstraction of a hydrogen atom by molecular oxygen or by the reaction of atomic hydrogen with molecular oxygen.

$$RH + O_2 \rightarrow R^{\bullet} + HO_2^{\bullet} \quad (1)$$

$$H^{\bullet} + O_2 + M \rightarrow HO_2^{\bullet} + M \quad (2)$$

The hydroperoxyl radical produced in the above sequence can either self-react or abstract a hydrogen atom generating hydrogen peroxide, which subsequently decomposes to produce two reactive hydroxyl radicals.

$$RH + HO_2^{\bullet} \rightarrow R^{\bullet} + H_2O_2 \quad (3)$$

$$HO_2^{\bullet} + HO_2^{\bullet} \rightarrow H_2O_2 + O_2 \quad (4)$$

$$H_2O_2 + M \rightarrow HO^{\bullet} + HO^{\bullet} + M \quad (5)$$

It has been shown[2,3] that changing the relative rates of (i) abstraction by the hydroperoxyl radical and (ii) its self-reaction either promotes in (i) or inhibits in (ii) the reactivity of a fuel. The self-reaction of hydroperoxyl radicals inhibits fuel reactivity because this reaction consumes hydroperoxyl radicals which could otherwise abstract a hydrogen atom from a stable species to ultimately produce two hydroxyl radicals from one hydroperoxyl radical, as depicted in the reactions above. As the temperature increases, the reaction of a hydrogen atom with molecular oxygen produces a hydroxyl radical via $H^{\bullet} + O_2 \rightarrow O^{\bullet} + HO^{\bullet}$, becoming the most dominant chain branching reaction at higher temperatures.[4]

* To whom correspondence should be addressed. E-mail: aguilera@chem-bio.uni-karlsruhe.de.
† Universität Karlsruhe.
‡ National University of Ireland.

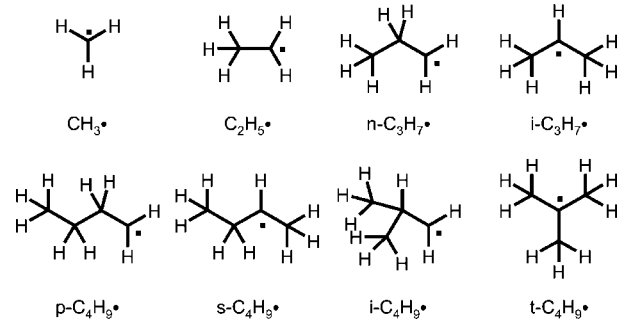

Figure 1. Set of radicals formed in $RH + HO_2^{\bullet} \rightarrow R^{\bullet} + H_2O_2$.

Despite this, there are very few reliable determinations of the rates of hydrogen atom abstraction from hydrocarbons by the hydroperoxyl radical; all of these were obtained from measurements in boric acid-coated static reactors by an indirect technique over a quite narrow range of temperatures;[5–9] most values have been estimated.[10–14]

Quantum chemical calculation can provide accurate structural and energetic data of small polyatomic molecules of relevance to inter alia combustion chemistry. Concerning reaction barriers for hydrogen abstractions, an overview of the performance of density functionals has been presented recently by Sousa et al.[15] The authors conclude that B3LYP performs poorly for such reactions. Vandeputte et al.[16] extensively studied the behavior of CBS-QB3[17] by calculating reaction barriers and reaction rates for hydrogen abstractions. They found very good agreement for the barrier height for the abstraction by methyl from methane, in comparison with a high-level W1 calculation. A much poorer result was found for the abstraction by methyl from ethene. In all the cases treated, the calculated reaction rate computed with CBS-QB3 was satisfactory in comparison with experimental reaction rates.

Our goal in this work is to compute the reaction barriers for the series of reaction of $HO_2^{\bullet}$ with methane, ethane, propane, *n*-butane, and iso-butane, see Figure 1, as studied by Carstensen

10.1021/jp8012464 CCC: $40.75 © 2008 American Chemical Society
Published on Web 07/08/2008

and co-workers,[18] at the CBS-QB3 level of theory. In our work, we use the CCSD(T) level in an attempt to obtain reaction barriers with chemical accuracy, that is, within ~4 kJ mol^{-1}, and obtain from them the reaction rates. Such accuracy can only be achieved by performing the CCSD(T) calculations in very large and nearly complete one-electron basis sets, followed by basis-set extrapolation or by expanding the coupled-cluster wave function in a many-electron basis that contains terms that depend explicitly on the interelectronic distances in the system.[19]

The general theory of the explicitly correlated coupled-cluster approach is described in detail by Noga et al.[20] and a number of review articles exist.[21–23] In 2000, the theory was extended to single-reference open-shell cases with unrestricted Hartree−Fock (UHF) and restricted open-shell Hartree−Fock (ROHF) reference determinants,[24,25] and illustrative applications of explicitly correlated coupled-cluster theory have been reported recently.[26–29]

This paper has the following structure: First, we present the computational details to obtain both the reaction barriers and the reaction rate constants. Then, we provide a benchmarking case to establish the accuracy of the methods employed. After that, the results for the reaction barriers, by applying the different methods under study, and the proposed Arrhenius-like expression along with the resulting reaction constants are presented. A detailed comparison with previous works, both experimental and computational, is shown. Finally, we propose reaction rate constants according to the carbon substitution, and the conclusions are presented.

2. Computational Details

Reaction Barriers. Geometry optimizations utilizing analytical nuclear gradients are carried out to locate minima and saddle points at the level of density functional theory (DFT) by using the B3LYP exchange-correlation functional[30–32] in combination with the def2-TZVP basis[33] as implemented in the Turbomole program.[34–39] Redundant internal coordinates are used for the geometry optimizations, and the search for saddle points is performed by using the trust radius image minimization approach.[40] Harmonic frequencies are calculated analytically for all species at the B3LYP/def2-TZVP level and are used unscaled throughout the work. The frequencies of the minima are all real, and the saddle points exhibit only one imaginary frequency.

Moreover, single-point energy calculations are carried out in the same basis by using the functionals BP86,[41,42] TPSS,[43] TPSSh,[44] BMK,[45] and B97K,[45] the compound methods CBS-QB3 and CBS-APNO[46] calculated with Gaussian,[47] and conventional spin-restricted coupled-cluster theory in the correlation-consistent triple-ζ basis (cc-pVTZ) of Dunning.[48] These spin-restricted coupled-cluster calculations are based on a spin-restricted Hartree−Fock reference (restricted Hartree−Fock, RHF, or ROHF) and are carried out with Molpro.[49] The coupled-cluster calculations include singles and doubles (RCCSD)[50] as well as perturbative triples [RCCSD(T)][51] and are performed in the frozen-core approximation.

In the detailed study of the $CH_4 + HO_2^{\bullet}$ system, the conventional coupled-cluster method with the family of *n*-tuple-ζ basis sets (cc-pV*n*Z), with $n = 2$, 3, 4, and 5, is used.[48] In this system, integral-direct explicitly correlated CCSD-R12 calculations are performed with the DIRCCR12-OS program[52,53] by using a spin-restricted Hartree−Fock reference wave function (RHF or ROHF). A spin-restricted coupled-cluster calculation is performed for the closed-shell systems, whereas the open-shell systems are treated at the spin-unrestricted coupled-cluster ROHF-CCSD-R12 level. For comparison, the conventional coupled-cluster calculations in the cc-pV*n*Z basis sets on this system are carried out similarly, that is, by using the ROHF-CCSD(T) method for the open shells. The CCSD-R12 calculations are carried out in the 19s14p8d6f4g3h basis (9s6p4d3f for H).[54] The perturbative triples are taken from the conventional coupled-cluster approach.

Reaction Rates. For the calculation of reaction rate constants, simple transition-state theory is used. Observed rates are of course dependent on the whole potential energy surface and not just on the reactants and the transition state, but it would be computationally too expensive to use some of the methodologies employed here for that purpose. The well-known expression for the reaction rate constant of a bimolecular reaction $X + Y \leftrightarrows XY^{\ddagger}$ is:[55]

$$k = \kappa V_m \frac{k_B T}{h} \frac{Q^{\ddagger}}{Q_X Q_Y} \exp\left(\frac{-\Delta E_{B,0}}{RT}\right) \quad (6)$$

where $Q^{\ddagger}$, Q_X, and Q_Y, are the dimensionless partition functions (including translational, vibrational, and rotational contributions) of the transition state and the reactants, respectively, calculated by using the module Freeh of Turbomole (by using the harmonic oscillator and the rigid rotor approximation and by correcting for internal hindered rotations). R is the gas constant, k_B is the Boltzmann constant, h is the Planck constant, and V_m is the molar volume of an ideal gas at temperature T, which varied from 600 to 1300 K in the present work. $\Delta E_{B,0}$ is the electronic barrier height $\Delta E_{B,e}$ plus the zero-point vibrational energy (ZPVE). The ZPVE is computed at the B3LYP/def2-TZVP level and is included for all the methods under study. κ is the transmission coefficient accounting for tunneling effects, computed from the well-known Wigner formula:[56]

$$\kappa = 1 - \frac{1}{24}\left(\frac{h\nu}{k_B T}\right)^2 \left(1 + \frac{RT}{\Delta E_{B,0}}\right) \quad (7)$$

Only the imaginary frequency, ν, associated with the reaction coordinate and the reaction barrier $\Delta E_{B,0}$ are required to calculate κ. For the temperature range of interest here, the Wigner formula does not yield transmission coefficients significantly different from those from the Eckart formula nor from the approach proposed by Skodje and Truhlar.[57] For example, for a prototypical system with $\nu = 1650$i cm^{-1} and $\Delta E_{B,0} = 90$ kJ mol^{-1}, which represents our systems well, Truhlar's approach and the Eckart formula give identical results in the temperature range 700−1300 K and are not more than 15% larger than the Wigner transmission coefficient. At 1300 K, $\kappa_{Wigner} = 1.16$ and $\kappa_{Eckart} = 1.15$, whereas at 700 K, $\kappa_{Wigner} = 1.51$ and $\kappa_{Eckart} = 1.71$, and only at lower temperatures, the differences become more pronounced, for example at 600 K, $\kappa_{Wigner} = 1.69$ and $\kappa_{Eckart} = 2.16$.

Corrections to account for hindered rotations are included for all rotations about the C−C and O−O bonds as well as for rotations about the reaction coordinate C···H···O. Following Vansteenkiste et al.,[58] instead of removing the harmonic vibrational modes from the partition function, we correct it by multiplying with the ratio q_{hr}/q_{v-1D}. To obtain q_{hr}, potential energy curves are computed for the rotations about the above-mentioned bonds by using discrete steps of 5°, thereby allowing for a geometry relaxation of all the other internal coordinates (for the transition state, the difference between the C···H and H···O distances is kept fixed because otherwise, the geometry relaxation would lead to either the reactants or the products). A one-dimensional Schrödinger equation is solved to obtain the eigenstates needed to compute the partition function q_{hr}. q_{v-1D} is the harmonic oscillator value obtained from these one-dimensional curves. The reactants and transition states have

several conformations, which are all accounted for by computing the hindered-rotor partition function with respect to rotation about 360°. This procedure, for example, yields a factor of 2 for the rotation about the O—O bond for the two conformations that cannot be superimposed by rotation.[59] Symmetry numbers are included in the hindered-rotor partition functions for symmetric groups such as $-CH_3$, but most of these factors cancel between reactant and transition state. In the reactions producing the radicals n-$C_3H_7^\bullet$, p-$C_4H_9^\bullet$, and i-$C_4H_9^\bullet$, however, the lower symmetry of the hindered rotation about one of the C—C bonds in the transition state adds a factor of 3 to the reaction rate. Similarly, in the reactions yielding the $CH_3^\bullet$ and t-$C_4H_9^\bullet$ radicals, symmetry numbers for the rotations of the methyl and tertiary-butyl groups in the transition state are not compensated by a corresponding symmetry number in the reactant. Moreover, a factor of 2 is included for the reaction producing s-$C_4H_9^\bullet$, because a chiral transition state is involved.[59] As a byproduct, the scanning procedure confirmed that the energy calculations were done for the lowest-energy conformers.

Arrhenius-like expressions of the form:

$$k = AT^n \exp\left(\frac{-E_A}{RT}\right) \tag{3}$$

are fitted to the computed rate constants at temperatures 600−1300 K (in 100 K intervals); A, n, and E_A are treated as fitting parameters. We fit the above expression to rate constants computed from the B3LYP/def2-TZVP partition functions (corrected for hindered rotations) with the best estimates of the reaction barriers $\Delta E_{B,0}$ obtained at the coupled-cluster level of theory (vide infra). Note that these best estimates are used not only in the exponential but also in the Wigner formula for the transmission coefficient κ.

In this section, we have shown the procedure used to calculate the rate constants. It mimics the one employed by Carstensen et al., except that we have used alternative methods to compute the reaction barrier. This allows us to focus on the differences arising from these contrasting approaches. Note that the consequences of using B3LYP geometries, albeit with different basis functions, which both Carstensen et al. and ourselves employ, are difficult to predict. To improve on this, one could optimize all of the geometries at the coupled-cluster level of theory, but even then, the overall accuracy will remain difficult to assess because of the approximations in the TST treatment.

3. Benchmarking

Before presenting and discussing the results for all the reactions, let us first have a close look at the barrier for the reaction:

$$CH_4 + HO_2^\bullet \rightarrow TS^\ddagger \rightarrow CH_3^\bullet + H_2O_2$$

For this reaction, we calculate the optimized geometries at the B3LYP/def2-TZVP level for the two reactants, the two products, and the transition state TS‡. The geometry of the latter can be seen in Figure 2. We can compare the C···H distance in the TS‡, 1.430 Å, with the same distance found in the CH_4 minimum, 1.090 Å. The H···O distance is 1.124 Å for the TS‡ and 0.968 Å for the H_2O_2 minimum. This indicates a TS‡ very close to the products, $CH_3^\bullet + H_2O_2$, and agrees with Hammond's postulate[60] with respect to the endothermic character of the reaction under study. The electronic energies are obtained at the level of ROHF-CCSD-R12 theory. This theory uses electronic wave functions that depend explicitly on all of the electron−electron distances and is capable of yielding results close to those that would be obtained in a complete basis set of atomic orbitals—if it were possible to use such a basis. To the CCSD-R12 energies, we add the perturbative (T) correction for connected triples computed in the cc-pV5Z basis, and we shall refer to the corresponding energies as CCSD(T)-R12 in short. Table 1 shows the electronic atomization energies for the five species involved in the above reaction, computed at this CCSD(T)-R12 level.

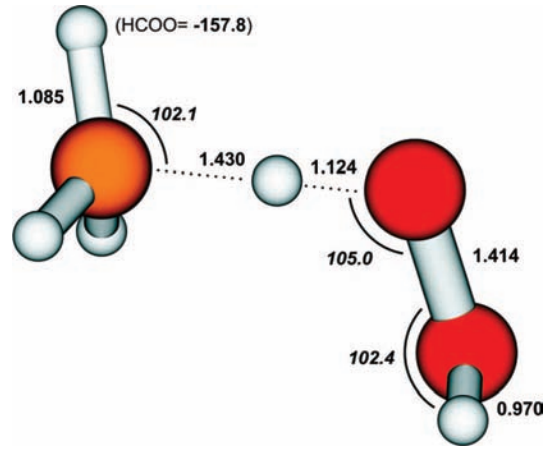

Figure 2. Geometry of the transition state of the $CH_4 + HO_2^\bullet$ reaction. Distances in angstroms and angles in degrees.

TABLE 1: Electronic Atomization Energies (kJ mol^{-1})

system	experiment[a]	calculation[b]
CH_4	1755.4	1752.5
$HO_2^\bullet$	732.5	729.9
TS‡		2372.6
$CH_3^\bullet$	1285.7	1283.0
H_2O_2	1122.1	1122.3

[a] Obtained from experimental atomization enthalpy at 0 K and experimental ZPVE from ref 66. [b] Obtained by adding the (T) triples correction from cc-pV5Z basis to the ROHF-CCSD(T)-R12 energies.

The CCSD(T)-R12 results agree to within 3 kJ mol^{-1} with well-known experimental data, and we expect that the atomization energy of TS‡, and thus the barrier height, is similarly accurate. This assumption is based both on our previous work with the explicitly correlated methods and the low multireference character of the system; the latter was observed as we performed a multireference study (CASSCF) on the transition state TS‡ and found that the wave function is dominated by a single determinant. The agreement with experiment is very satisfactory. We should note that the seemingly extreme accuracy for H_2O_2 is a coincidence, because several corrections have been omitted. To obtain a better founded agreement, it would be necessary to include higher excitations into the coupled-cluster treatment (full triples as well as quadruples and quintuples), to include core orbitals into the correlation treatment, and to correct for relativistic and non-Born−Oppenheimer effects,[61,62] but because of the amount of computational time required, they are beyond the scope of this work.

The electronic reaction energy, $\Delta E_{R,e}$, and the electronic barrier height, $\Delta E_{B,e}$, can be calculated from the CCSD(T)-R12 data displayed in Table 1. We compare the CCSD(T)-R12 data with the results obtained from conventional CCSD(T) theory using the standard cc-pVnZ basis sets. Table 2 shows the computed data ($\Delta E_{R,e}$ and $\Delta E_{B,e}$) obtained with the conventional CCSD(T) method in the cc-pVnZ basis sets. The results show clearly that CCSD(T) calculations in small basis sets such as cc-pVDZ and cc-pVTZ are not accurate enough for our

TABLE 2: Reaction Energy, $\Delta E_{R,e}$, and Reaction Barrier, $\Delta E_{B,e}$, for $CH_4 + HO_2^{\bullet} \rightarrow CH_3^{\bullet} + H_2O_2$ (kJ mol^{-1})[a]

basis	$\Delta E_{R,e}$	$\Delta E_{B,e}$
cc-pVDZ	94.5	124.0
cc-pVTZ	81.9	113.5
cc-pVQZ	79.1	111.5
cc-pV5Z	77.9	110.5
cc-pV(Q5)Z[b]	77.0	109.6
CCSD(T)-R12	77.2	109.9

[a] Electronic contribution from ROHF-CCSD(T) calculations. [b] Extrapolated from the cc-pVQZ and cc-pV5Z basis sets by using the n^{-3} formula of Helgaker et al.[63]

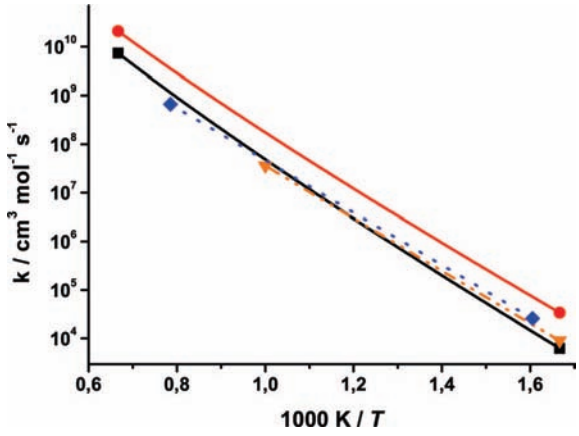

Figure 3. $k(CH_4 + HO_2^{\bullet} \rightarrow CH_3^{\bullet} + H_2O_2)$. This work (—■—), Carstensen[18] (—●—), Baulch[10] (-··▼··-), Baldwin[6] (···◆···).

purposes. The deviations from the CCSD(T)-R12 values are 14−17 and 4−-5 kJ mol^{-1}, respectively. Only in the case of the cc-pVQZ basis is the error below 3 kJ mol^{-1}.

Because the convergence of the computed data with the size of the atomic basis set is slow but systematic, it is possible to extrapolate the results to the limit of a complete basis (cc-pV∞Z) by using the cc-pVQZ and cc-pV5Z values;[63] such an extrapolation yields energies that are only 0.2−0.3 kJ mol^{-1} away from the CCSD(T)-R12 data. This is a strong indication that both methods are accurate within 1 kJ mol^{-1} of the basis-set limit of CCSD(T) theory.

4. Results

Reaction Barriers. At present, it is possible to perform frozen-core CCSD-R12 calculations on the transition state of the reaction of CH_4 with the $HO_2^{\bullet}$ radical in the large 19s14p8d6f4g3h basis (9s6p4d3f for H), but similar calculations on the transition states for the reactions with the larger hydrocarbons are technically not feasible. Therefore, we have calculated the electronic barrier heights for all the reactions in the def2-TZVP basis by using various functionals and in the cc-pVTZ basis set by using frozen-core RCCSD(T) theory.

For the reaction of the hydroperoxyl radical with methane, the B3LYP/def2-TZVP ZPVE correction to the barrier (applied to all the methods) amounts to −9.8 kJ mol^{-1}. Adding this contribution to the ROHF-CCSD(T)/cc-pVTZ and CCSD(T)-R12 electronic barriers (cf. Table 2) yields $\Delta E_{B,0}$ = 103.7 kJ mol^{-1} and $\Delta E_{B,0}$ = 100.1 kJ mol^{-1}, respectively. Thus, the CCSD(T)/cc-pVTZ value appears to slightly overestimate the $CH_4 + HO_2^{\bullet}$ barrier height. This can be easily corrected by scaling the electron-correlation contribution to the electronic barrier $\Delta E_{B,0}$ by a factor of 1.053. This factor is the ratio between the correlation contribution in the R12 and cc-pVTZ basis sets. Note that the electron-correlation contribution to the barrier is negative. We adopt this scaling factor of 1.053 to obtain the best estimates of the barrier heights for all the reactions under study. Note also that because the factor applies only to the correlation contribution, $\Delta E_{B,0}$ calculated by using CCSD(T)-R12 is not equal to the best estimate (100.1 versus 100.4 kJ mol^{-1}) because of the different basis set used in the noncorrelation contribution but allows us to be consistent in the treatment of all the reactions under study. Therefore, all of them are computed at the same level. The results are presented in Table 3, with the best estimates given in the last row.

TABLE 3: Reaction Barriers $\Delta E_{B,0}$, for the Reactions of the Hydrocarbons with the Hydroperoxyl Radical (kJ mol^{-1})[a]

method[a]	$CH_3^{\bullet}$	$C_2H_5^{\bullet}$	n-$C_3H_7^{\bullet}$	i-$C_3H_7^{\bullet}$	p-$C_4H_9^{\bullet}$	s-$C_4H_9^{\bullet}$	i-$C_4H_9^{\bullet}$	t-$C_4H_9^{\bullet}$
B3LYP[b]	97.6	78.2	79.5	64.5	78.9	64.3	79.2	54.3
BP86	75.0	53.6	55.9	39.0	55.2	38.9	55.7	28.5
TPSS	86.2	65.5	66.7	50.8	65.6	51.0	66.2	39.9
TPSSh	94.9	75.4	76.3	61.4	75.4	61.7	76.0	51.4
BMK	112.4	92.1	95.5	80.2	92.9	78.9	92.8	69.8
B97K	114.7	96.2	97.5	82.9	97.0	82.6	96.3	72.7
CBS-QB3	92.6	74.0	71.4	59.4	71.0	57.2	72.2	48.5
CBS-APNO	98.5	79.0	76.3	64.1	75.6	61.9	77.2	53.8
RCCSD(T)[c]	104.0	86.0	86.4	72.3	85.9	69.6	83.6	62.6
best estimate[d]	100.4	81.6	82.0	67.3	81.4	64.4	79.0	57.2

[a] All methods include B3LYP ZPVE. [b] All DFT data are obtained in the def2-TZVP basis. [c] Frozen-core CCSD(T)/cc-pVTZ value. [d] Best estimate of the barrier height $\Delta E_{B,0}$ obtained by scaling the frozen-core CCSD(T)/cc-pVTZ electron-correlation contributions to $\Delta E_{B,e}$ by a factor of 1.053 (see text).

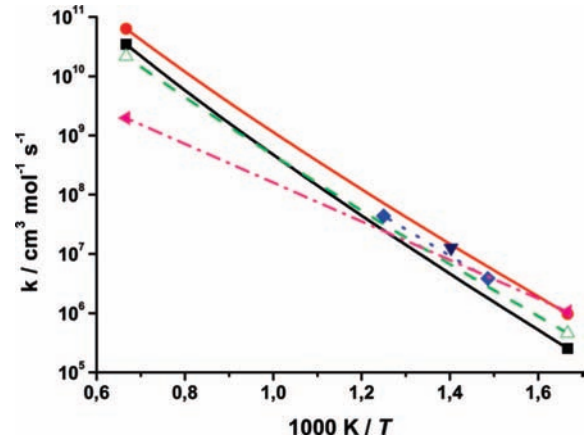

Figure 4. $k(C_2H_6 + HO_2^{\bullet} \rightarrow C_2H_5^{\bullet} + H_2O_2)$. This work (—■—), Carstensen[18] (—●—), Scott[8] (--Δ--), Baldwin[5] (···▼···), Baldwin[9] (▼), Tsang[12] (-··-).

In comparison with the DFT results obtained with various functionals, we find that the B3LYP values are very close to the best estimates. On average, the B3LYP barriers are only 3 kJ mol^{-1} below the best estimates. The TPSSh functional yields values that in turn are about 3 kJ mol^{-1} below the B3LYP barriers. Furthermore, the BMK and B97K functionals yield barriers that are too high in comparison with the best estimates derived from CCSD(T) calculations. These functionals overestimate the barriers by more than 10 kJ mol^{-1}.

The results (using the B3LYP values) show, not unexpectedly, that the reaction barriers for the abstraction of a primary hydrogen cluster is around 79 kJ mol^{-1}, that for the abstraction of a secondary hydrogen is lower at about 64 kJ mol^{-1}, and finally that for the abstraction of a tertiary hydrogen is lower again at 54 kJ mol^{-1}—reflecting of course the decrease in the C—H bond dissociation energies from primary to tertiary.[64]

A more detailed look should be taken at the results of the compound methods CBS-QB3 and CBS-APNO. As can be

TABLE 4: Calculated TST Rate Constants (for a Selection of Temperatures, $cm^3\ mol^{-1}\ s^{-1}$) Coming from the Fit Parameters A ($cm^3\ mol^{-1}\ s^{-1}$), n, E_A ($kJ\ mol^{-1}$), and Imaginary Frequency ν (cm^{-1})

radical	600 K	800 K	1000 K	1200 K	A	n	E_A	ν
$CH_3^\bullet$	6.16×10^3	1.48×10^6	4.79×10^7	5.52×10^8	11.3	3.74	87.9	1539i
$C_2H_5^\bullet$	2.54×10^5	2.49×10^7	4.69×10^8	3.75×10^9	34.6	3.61	70.8	1661i
n-$C_3H_7^\bullet$	1.94×10^5	2.10×10^7	4.21×10^8	3.53×10^9	13.5	3.75	71.9	1656i
i-$C_3H_7^\bullet$	1.15×10^6	5.59×10^7	6.83×10^8	4.05×10^9	58.1	3.37	58.2	1684i
p-$C_4H_9^\bullet$	2.14×10^5	2.24×10^7	4.37×10^8	3.55×10^9	101.9	3.48	72.9	1657i
s-$C_4H_9^\bullet$	3.60×10^6	1.63×10^8	1.91×10^9	1.11×10^{10}	109.1	3.40	56.6	1677i
i-$C_4H_9^\bullet$	2.94×10^5	3.00×10^7	5.75×10^8	4.63×10^9	116.5	3.49	72.3	1648i
t-$C_4H_9^\bullet$	5.89×10^6	1.78×10^8	1.59×10^9	7.57×10^9	650.4	3.01	50.6	1658i

extracted from Table 3, the standard deviation of the CBS-QB3 method is more than 8 kJ mol^{-1}. By taking into account that this is the difference to the coupled-cluster basis-set limit, and as we pointed out earlier, this has an error against experiment of at least 3 kJ mol^{-1}, it would potentially lead to an error of more than 10 kJ mol^{-1}. As is perhaps to be expected, the CBS-APNO method performs very closely to our best estimates because of the additional corrections that embodies over those in CBS-QB3 and which therefore bring it nearer to the CCSD(T) basis-set limit.

Preliminary work[65] on H-abstraction from *n*-butanol by $HO_2^\bullet$ may be compared to our results for *n*-butane. The barrier heights evaluated at the CBS-QB3 and CBS-APNO levels of theory for abstraction from the terminal or δ-carbon in the alcohol (70.3 and 75.0 kJ mol^{-1}, respectively) are very close to those reported here for abstraction of the primary hydrogens in *n*-butane (Table 3). This is not unexpected, given the diminishing influence of the hydroxyl group along the lengthening carbon chain. The influence of the –OH group becomes evident in the comparison of the barrier heights for abstraction of a secondary H from *n*-butane and a secondary H from the γ position in *n*-butanol, which might be expected to be sufficiently far from the –OH group to behave similarly to its alkane equivalent. However, the difference in this case between the barrier heights for *n*-butanol and *n*-butane is noticeable, though small (ca. 4 kJ mol^{-1} lower for *n*-butanol, with CBS-QB3 and CBS-APNO barriers of 53.5 and 58.4 kJ mol^{-1}, respectively) and is attributable to a stabilization of the transition state due to a H-bonding interaction between the H of the –OH group and the terminal O of $HO_2^\bullet$.

Reaction Rates. The final kinetic results are collected in Table 4 where we present the TST rate constants k calculated from the fitting by using the B3LYP/def2-TZVP partition functions in conjunction with the best estimates of $\Delta E_{B,0}$. The fit parameters A, n, and E_A needed to represent the rate constants by an Arrhenius-like expression are also given in Table 4. Note that the activation energy E_A given in the table is the fit parameter, not the best estimate $\Delta E_{B,0}$. In fact, the fitted E_A values are about 7−14 kJ mol^{-1} lower than the best estimates.

5. Comparison with Previous Work

In this section, we compare the rate constants obtained in the present work with those obtained in previous studies. We can divide these works in three categories.

• Purely theoretical work. This includes our work and the one done by Carstensen et al.[18] The approaches differ drastically in the computation of the reaction barrier. Carstensen et al.[18] provide reaction rates by using the CBS-QB3 method. The reaction barriers are not explicitly shown in the cited reference; therefore, we compute the CBS-QB3 values in our study. In Table 3, we can see that our best estimate is always higher than that obtained with CBS-QB3. This means that we expect our rate constant to be always slower. Because the reaction barrier appears in $\exp(-\Delta E_{B,0}/RT)$, the effect of the difference in reaction barrier on the reaction rates will be significant at low and medium temperatures (where the reactions under study play a key role) and less important at high temperatures. For example, if the difference in the calculated reaction barriers is 10 kJ mol^{-1}, at 530 K, the difference in the reaction rate coming from the exponential part is of an order of magnitude, and it is only a factor of 2 at 1760. We confirm these effects through all the figures in this section.

• Literature review. We include here the extensive literature reviews of Tsang et al.[12,13] and that of Orme et al.,[14] which were carried out in order to construct detailed chemical kinetic models.

• Experimental work. There are no direct measurements of the reactions involved. The work done by Baldwin et al.[5,6,9,11] is based on the measurement of relative reaction rates of the reaction in question by the use of a reference reaction.

Methane. Our values are in excellent agreement with the relative rate measurements (based on $HO_2^\bullet + HO_2^\bullet \rightarrow H_2O_2 + O_2$) of Baldwin et al.[6] and the recommendation of Baulch et al.[10] However, our values are between five times (at 600 K) and three times (at 1500 K) slower compared to those of Carstensen et al.[18] (Figure 3).

Ethane. Our rate constants are two times slower than the relative rate measurements of Baldwin et al.[5] and show a stronger temperature curvature compared to the previous recommendations of Scott and Walker[8] and the review of Tsang et al.[12] and thus are considerably faster at temperatures above 600 K. Our rate constant is four times slower than that calculated by Carstensen et al.[18] at 600 K and is twice as slow at 1500 K (Figure 4).

Propane. In the case of propane, there are two distinct abstractable hydrogen atoms leading to either *n*-propyl (Figure 5) or iso-propyl (Figure 6) radicals.

Baldwin et al.[11] performed a relative rate measurement at 773 K and found a relative rate of 0.03 for the production of the *n*-propyl radical relative to the reaction $CH_2O + HO_2^\bullet \rightarrow HCO^\bullet + H_2O_2$. All other rate constants presented in Figure 5 are either calculations or estimates. The rate constant calculated in this study is in very good agreement with all other estimations, slightly slower at 600 K. The value calculated by Carstensen et al.[18] is more than five times faster at 600 K but very similar at 1500 K.

Baldwin et al.[11] also carried out a relative rate measurement for the production of the iso-propyl radical at 773 K and found a relative rate of 0.048 relative to the reaction $CH_2O + HO_2^\bullet \rightarrow HCO^\bullet + H_2O_2$. All other rate constants presented in Figure 6 are also either calculations or estimates. The rate constant calculated in the present study is in very good agreement with the determination of Baldwin et al. and with the recommendations of Scott and Walker[8] and Orme et al.[14] However, our

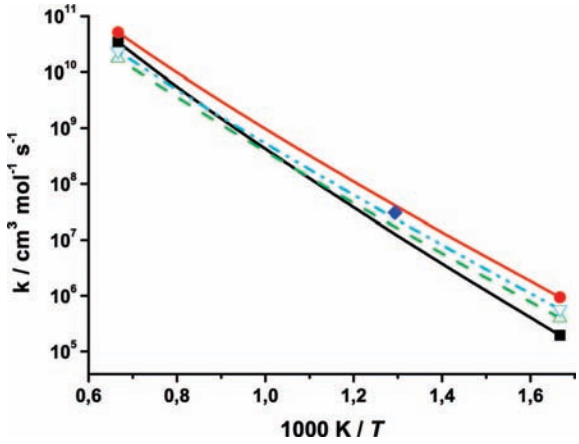

Figure 5. $k(C_3H_8 + HO_2^{\bullet} \rightarrow n\text{-}C_3H_7^{\bullet} + H_2O_2)$. This work (—■—), Carstensen[18] (—●—), Scott[8] (--Δ--), Orme[14] (-•••▽-•••), Baldwin[11] (◆).

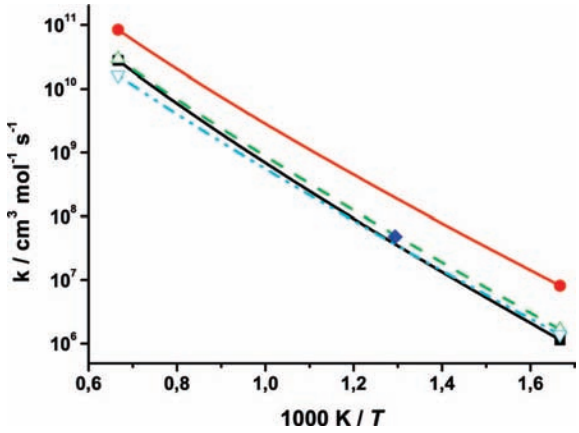

Figure 6. $k(C_3H_8 + HO_2^{\bullet} \rightarrow i\text{-}C_3H_7^{\bullet} + H_2O_2)$. This work (—■—), Carstensen[18] (—●—), Scott[8] (--Δ--), Orme[14] (-•••▽-•••), Baldwin[11] (◆).

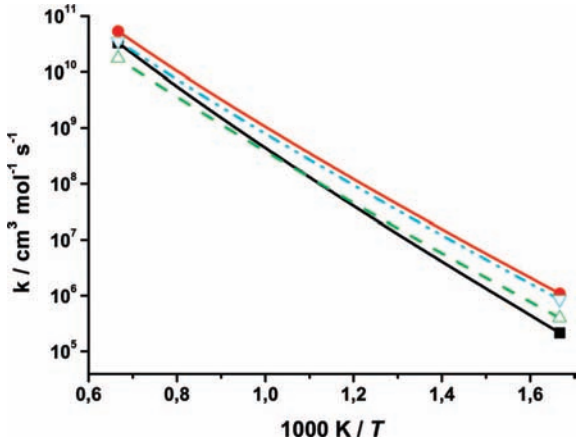

Figure 7. $k(n\text{-}C_4H_{10} + HO_2^{\bullet} \rightarrow p\text{-}C_4H_9^{\bullet} + H_2O_2)$. This work (—■—), Carstensen[18] (—●—), Scott[8] (--Δ--), Orme[14] (-•••▽-•••).

calculation is significantly slower than that computed by Carstensen et al.[18]

***n*-Butane.** In the case of *n*-butane, both primary or secondary radicals can be generated (Figures 7 and 8).

There have been no measurements of the rate constant for hydrogen atom abstraction by the hydroperoxyl radical from *n*-butane. The rate constant calculated in our study is again in very good agreement with all other estimations, consistent with the result for abstraction of a primary hydrogen atom from

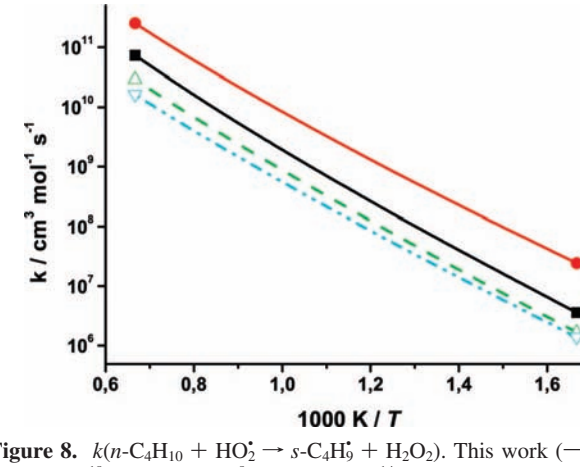

Figure 8. $k(n\text{-}C_4H_{10} + HO_2^{\bullet} \rightarrow s\text{-}C_4H_9^{\bullet} + H_2O_2)$. This work (—■—), Carstensen[18] (—●—), Scott[8] (--Δ--), Orme[14] (-•••▽-•••).

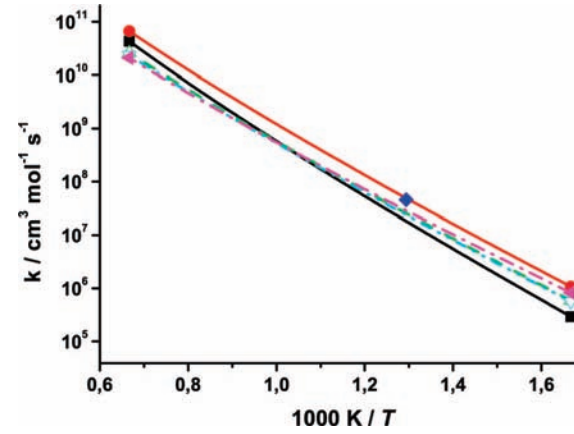

Figure 9. $k(i\text{-}C_4H_{10} + HO_2^{\bullet} \rightarrow i\text{-}C_4H_9^{\bullet} + H_2O_2)$. This work (—■—), Carstensen[18] (—●—), Scott[8] (--Δ--), Orme[14] (-•••▽-•••), Baldwin[11] (◆), Tsang[13] (-•••-).

propane. The rate constant calculated by Carstensen et al.[18] is five times faster at 600 K but very close at 1500 K.

For secondary hydrogen atom abstraction from butane, our calculations are two times faster than the recommendations of Scott and Walker. The rate constant calculated by Carstensen et al.[18] is between seven times (600 K) and three times (1500 K) faster than our calculation.

iso-Butane. For iso-butane, both iso-butyl (Figure 9) and tertiary-butyl (Figure 10) radicals are formed. Baldwin et al.[11] performed a relative measurement at 773 K and found a relative rate of 0.133 for the production of iso-butyl radicals relative to the reaction $CH_2O + HO_2^{\bullet} \rightarrow HCO^{\bullet} + H_2O_2$. Recommendations of Scott and Walker,[8] Orme et al.,[14] and Tsang[13] and the calculations of Carstensen et al.[18] are in reasonable agreement with this rate constant. Our calculation is 2−3 times slower than the value derived by Baldwin et al.[11] at 773 K.

Figure 10 depicts rate constants for the abstraction of the tertiary hydrogen atom from iso-butane. Baldwin et al.[11] performed measurements at 773 K and found a relative rate of 0.045 for the production of tert-butyl radicals relative to $CH_2O + HO_2^{\bullet} \rightarrow HCO^{\bullet} + H_2O_2$. Recommendations of Scott and Walker,[8] Orme et al.,[14] and Tsang[13] are in reasonable agreement with this rate constant. Our calculation is in excellent agreement with that of Baldwin et al.[11] At the same temperature, the value suggested by Carstensen et al.[18] is five times faster than that of Baldwin et al.[11]

Recommended Rate Constants. By using the data obtained in the previous section, we suggest values for the rate constants

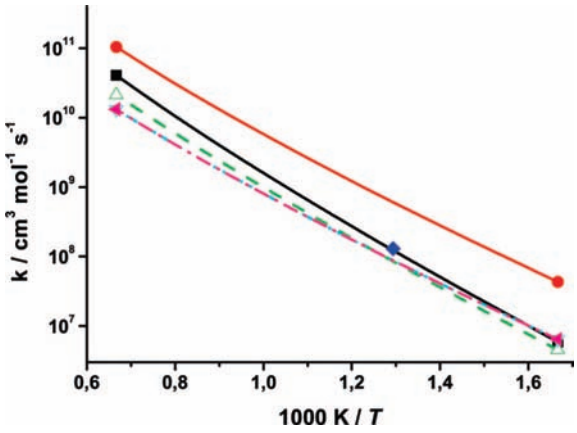

Figure 10. $k(i\text{-}C_4H_{10} + HO_2^{\bullet} \rightarrow t\text{-}C_4H_9^{\bullet} + H_2O_2)$. This work (—■—), Carstensen[18] (—●—), Scott[8] (--Δ--), Orme[14] (-•••▽-•••), Baldwin[11] (◆), Tsang[13] (-•••-).

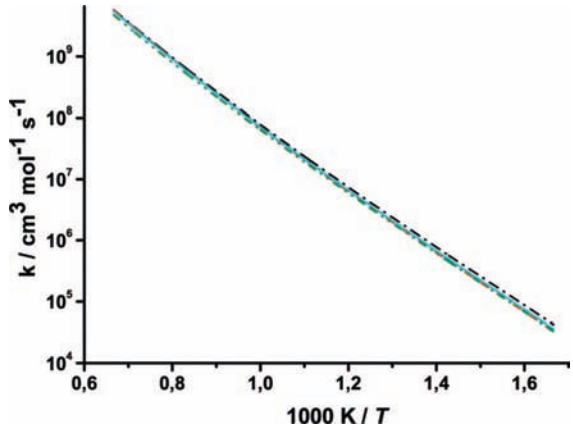

Figure 11. k for primary carbon on a per H-atom basis. $C_2H_5^{\bullet}$ (-•-), $n\text{-}C_3H_7^{\bullet}$ (- - -), $p\text{-}C_4H_9^{\bullet}$ (•••), $i\text{-}C_4H_9^{\bullet}$ (-- •••), average (—).

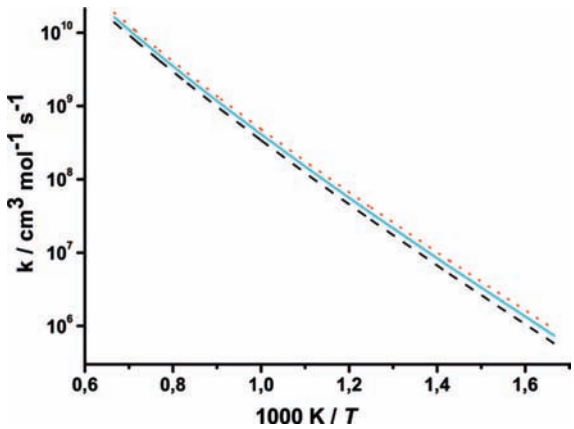

Figure 12. k for secondary carbon on a per H-atom basis. $i\text{-}C_3H_7^{\bullet}$ (- - -), $s\text{-}C_4H_9^{\bullet}$ (•••), average (—).

which depend upon the local environment of the hydrogen being abstracted, that is, whether from a primary, secondary, or tertiary carbon. In Figure 11, the rate constants for primary carbons are plotted separately, together with the resulting average. The same procedure is shown in Figure 12, in this case, for the secondary carbons. Note that these are rate constants on a per-hydrogen atom basis with the final suggested values summarized in Table 5.

6. Conclusions

We have computed the reaction barrier for the $CH_4 + HO_2^{\bullet}$ reaction within chemical accuracy by using R12 methodology.

TABLE 5: Fit Parameters A (cm ^{3} mol $^{-1}$ s $^{-1}$), n, E_A (kJ mol $^{-1}$) per Hydrogen Atom According to Carbon Type

carbon	A	n	E_A
$CH_3^{\bullet}$	2.8	3.74	87.9
primary	6.8	3.59	71.8
secondary	31.6	3.37	57.4
tertiary	650.4	3.01	50.6

Comparisons with results obtained with compound methods revealed that CBS-QB3 may be insufficient to achieve the same goal. Methods higher in the CBS hierarchy such as CBS-APNO should be used for high accuracy. We have computed the rate constants for the reactions under study, and we have used them to recommend values for various substitutions of the carbon involved in the reaction. We have compared the constants computed in the present work with available experimental data and found a reasonable agreement for methane, primary, secondary, and tertiary carbons. In the comparison with previous theoretical work, we have found for all the molecules in the study lower reaction rates, which is a reasonable consequence of our higher reaction barriers.

Acknowledgment. This work was supported by the Deutsche Forschungsgemeinschaft, in an initial stage of the work through the Sonderforschungsbereich 551 "Carbon from the Gas Phase: Elementary Reactions, Structures, Materials" and in a later stage through Project no. KL 721/3-1. This work was further supported by the European Commission through a Transfer-of-Knowledge grant, MKTD-CT-2004−517248, with computational resources provided by the Irish Centre for High End Computing, ICHEC. We thank M. Olzmann and O. Welz for making available their program for computing corrections to the partition function due to hindered rotations.

References and Notes

(1) Simmie, J. M. *Prog. Energy Combust. Sci.* **2003**, *29*, 599.
(2) Curran, H. J.; Gaffuri, P.; Pitz, W. J.; Westbrook, C. K. *Combust. Flame* **1998**, *114*, 149.
(3) Curran, H. J.; Gaffuri, P.; Pitz, W. J.; Westbrook, C. K. *Combust. Flame* **2002**, *129*, 253.
(4) Westbrook, C. K. *Proc. Combust. Inst.* **2000**, *28*, 1563.
(5) Baldwin, R. R.; Dean, C. E.; Honeyman, M. R.; Walker, R. W. *J. Chem. Soc. Faraday Trans.* **1986**, *1*, 89.
(6) Baldwin, R. R.; Jones, P. N.; Walker, R. W. *J. Chem. Soc. Faraday Trans.* **1988**, *2*, 199.
(7) Handford-Styring, S. M.; Walker, R. W. *Phys. Chem. Chem. Phys.* **2001**, *3*, 2043.
(8) Scott, M.; Walker, R. W. *Combust. Flame* **2002**, *129*, 365.
(9) Baldwin, R. R.; Walker, R. W. *Symp. Int. Combust. Proc.* **1979**, *17*, 525.
(10) Baulch, D. L.; Cobos, C. J.; Cox, R. A.; Esser, C.; Frank, P.; Just, T. H.; Kerr, J. A.; Pilling, M. J.; Troe, J.; Walker, R. W.; Warnatz, J. *J. Phys. Chem. Ref. Data* **1992**, *21*, 411.
(11) Baldwin, R. R.; Fuller, A. R.; Longthorn, D.; Walker, R. W. In *Combustion Institute European Symposium*; Weinberg, F. J. Ed.; Academic Press: London, 1973; 1−70.
(12) Tsang, W.; Hampson, R. F. *J. Phys. Chem. Ref. Data* **1986**, *15*, 1087.
(13) Tsang, W. *J. Phys. Chem. Ref. Data* **1990**, *19*, 1.
(14) Orme, J. P.; Curran, H. J.; Simmie, J. M. *J. Phys. Chem. A* **2006**, *110*, 114.
(15) Sousa, S. F.; Fernandes, P. A.; Ramos, M. J. *J. Phys. Chem. A* **2007**, *111*, 10439.
(16) Vandeputte, A. G.; Sabbe, M. K.; Reyniers, M.-F.; Van Speybroeck, V.; Waroquier, M.; Marin, G. B. *J. Phys. Chem. A* **2007**, *111*, 11771.
(17) Montgomery, J. A., Jr.; Ochterski, J. W.; Petersson, G. A. *J. Chem. Phys.* **1994**, *101*, 5900.
(18) Carstensen, H.-H.; Dean, A. M.; Deutschmann, O. *Proc. Combust. Inst.* **2007**, *31*, 149.
(19) Noga, J.; Klopper, W.; Kutzelnigg, W. *Chem. Phys. Lett.* **1992**, *199*, 497.
(20) Noga, J.; Kutzelnigg, W. *J. Chem. Phys.* **1994**, *101*, 7738.

(21) Noga, J.; Klopper, W.; Kutzelnigg, W. In *Recent Advances in Computational Chemistry*; Barlett,R.J. Ed.; World Scientific: Singapore, 1997; Vol. 3.

(22) Noga, J.; Valiron, P. In *Computational Chemistry: Reviews of Current trends*; Leszcynski, J. Ed.; World Scientific: Singapore, 2002; Vol. 7.

(23) Klopper, W.; Noga, J. In *Explicitly Correlated Wave Functions in Chemistry and Physics*; Rychlewski, J. Ed.; Kluwer: Dordrecht, 2003.

(24) Noga, J.; Valiron, P. *Chem. Phys. Lett.* **2000**, *324*, 166.

(25) Noga, J.; Valiron, P.; Klopper, W. *J. Chem. Phys.* **2001**, *115*, 2022; 5690. Noga, J.; Valiron, P.; Klopper, W. *J. Chem. Phys.* **2002**, *117*, 2989, Erratum.

(26) Tew, D. P.; Klopper, W.; Heckert, M.; Gauss, J. *J. Phys. Chem. A* **2007**, *111*, 11242.

(27) Heckert, M.; Kállay, M.; Tew, D. P.; Klopper, W.; Gauss, J. *J. Chem. Phys.* **2006**, *125*, 044108.

(28) Klopper, W.; Noga, J. *ChemPhysChem* **2003**, *4*, 32.

(29) Aguilera-Iparraguirre, J.; Boese, A. D.; Klopper, W.; Ruscic, B. *Chem. Phys.* **2008**, *346*, 56.

(30) Becke, A. D. *J. Chem. Phys.* **1993**, *98*, 5648.

(31) Stephens, P. J.; Devlin, F. J.; Chabalowski, C. F.; Frisch, M. J. *J. Phys. Chem.* **1994**, *98*, 11623.

(32) Lee, C.; Yang, W.; Parr, R. G. *Phys. Rev. B* **1988**, *37*, 785.

(33) Weigend, F.; Ahlrichs, R. *Phys. Chem. Chem. Phys.* **2005**, *7*, 3297.

(34) *Turbomole version 5.9.1*; Turbomole GmbH: Karlsruhe, 2007; www.turbomole.com.

(35) Ahlrichs, R.; Bär, M.; Häser, M.; Horn, H.; Kölmel, C. *Chem. Phys. Lett.* **1989**, *162*, 165.

(36) Treutler, O.; Ahlrichs, R. *J. Chem. Phys.* **1995**, *102*, 346.

(37) Eichkorn, K.; Treutler, O.; Öhm, H.; Häser, M.; Ahlrichs, R. *Chem. Phys. Lett.* **1995**, *242*, 652.

(38) Deglmann, P.; Furche, F.; Ahlrichs, R. *Chem. Phys. Lett.* **2002**, *362*, 511.

(39) Unterreiner, B. V.; Sierka, M.; Ahlrichs, R. *Phys. Chem. Chem. Phys.* **2004**, *6*, 4377.

(40) Helgaker, T. *Chem. Phys. Lett.* **1991**, *182*, 503.

(41) Perdew, J. P. *Phys. Rev. B* **1986**, *33*, 8822.

(42) Becke, A. D. *Phys. Rev. A* **1988**, *38*, 3098.

(43) Tao, J.; Perdew, J. P.; Staroverov, V. N.; Scuseria, G. E. *Phys. Rev. Lett.* **2003**, *91*, 146401.

(44) Staroverov, V. N.; Scuseria, G. E.; Tao, J.; Perdew, J. P. *J. Chem. Phys.* **2003**, *119*, 12129. Staroverov, V. N.; Scuseria, G. E.; Tao, J.; Perdew, J. P. *J. Chem. Phys.* **2004**, *121*, 11507, Erratum.

(45) Boese, A. D.; Martin, J. M. L. *J. Chem. Phys.* **2004**, *121*, 3405.

(46) Ochterski, J. W.; Petersson, G. A.; Montgomery, J. A., Jr. *J. Chem. Phys.* **1996**, *104*, 2598.

(47) Frisch, M. J.; Trucks, G. W.; Schlegel, H. B.; Scuseria, G. E.; Robb, M. A.; Cheeseman, J. R.; Montgomery, J. A., Jr.; Vreven, T.; Kudin, K. N.; Burant, J. C.; Millam, J. M.; Iyengar, S. S.; Tomasi, J.; Barone, V.; Mennucci, B.; Cossi, M.; Scalmani, G.; Rega, N.; Petersson, G. A.; Nakatsuji, H.; Hada, M.; Ehara, M.; Toyota, K.; Fukuda, R.; Hasegawa, J.; Ishida, M.; Nakajima, T.; Honda, Y.; Kitao, O.; Nakai, H.; Klene, M.; Li, X.; Knox, J. E.; Hratchian, H. P.; Cross, J. B.; Bakken, V.; Adamo, C.; Jaramillo, J.; Gomperts, R.; Stratmann, R. E.; Yazyev, O.; Austin, A. J.; Cammi, R.; Pomelli, C.; Ochterski, J. W.; Ayala, P. Y.; Morokuma, K.; Voth, G. A.; Salvador, P.; Dannenberg, J. J.; Zakrzewski, V. G.; Dapprich, S.; Daniels, A. D.; Strain, M. C.; Farkas, O.; Malick, D. K.; Rabuck, A. D.; Raghavachari, K.; Foresman, J. B.; Ortiz, J. V.; Cui, Q.; Baboul, A. G.; Clifford, S.; Cioslowski, J.; Stefanov, B. B.; Liu, G.; Liashenko, A.; Piskorz, P.; Komaromi, I.; Martin, R. L.; Fox, D. J.; Keith, T.; Al-Laham, M. A.; Peng, C. Y.; Nanayakkara, A.; Challacombe, M.; Gill, P. M. W.; Johnson, B.; Chen, W.; Wong, M. W.; Gonzalez, C.; Pople, J. A. *Gaussian 03*, revision C.02; Gaussian, Inc.: Wallingford, CT, 2004.

(48) Dunning, T. H., Jr. *J. Chem. Phys.* **1989**, *90*, 1007.

(49) Werner, H.-J.; Knowles, P. J.; Lindh, R.; Manby, F. R.; Schütz, M.; Celani, P.; Korona, T.; Rauhut, G.; Amos, R. D.; Bernhardsson, A.; Berning, A.; Cooper, D. L.; Deegan, M. J. O.; Dobbyn, J.; Eckert, F.; Hampel, C.; Hetzer, G.; Lloyd, A. W.; McNicholas, S. J.; Meyer, W.; Mura, M. E.; Nicklass, A.; Palmieri, P.; Pitzer, R.; Schumann, U.; Stoll, H.; Stone, A. J.; Tarroni, R.; Thorsteinsson, T. *Molpro 2006.1.*; Cardiff: UK, 2006; www.molpro.net.

(50) Hampel, C.; Peterson, K.; Werner, H.-J. *Chem. Phys. Lett.* **1992**, *190*, 1.

(51) Deegan, M. J. O.; Knowles, P. J. *Chem. Phys. Lett.* **1994**, *227*, 321.

(52) Klopper, W.; Noga, J. *J. Chem. Phys.* **1995**, *103*, 6127.

(53) Noga, J.; Klopper, W.; Helgaker, T.; Valiron, P. http://www-laog.obs.ujf-grenoble.fr/valiron/ccr12/.

(54) Klopper, W.; Samson, C. C. M. *J. Chem. Phys.* **2002**, *116*, 6397.

(55) McQuarrie, D. A.; Simon, J. D. *Physical Chemistry: A Molecular Approach*; University Science Books: Sausalito, 1997.

(56) Steinfeld, J. I.; Francisco, J. S.; Hase, W. L. *Chemical Kinetics and Dynamics*, 2nd ed.; Prentice Hall: New York, 1999.

(57) Skodje, R. T.; Truhlar, D. G. *J. Phys. Chem.* **1981**, *85*, 624.

(58) Vansteenkiste, P.; van Neck, D.; VanSpeybroeck, V.; Waroquier, M. *J. Chem. Phys.* **2006**, *124*, 044314. Vansteenkiste, P.; van Neck, D.; VanSpeybroeck, V.; Waroquier, M. *J. Chem. Phys.* **2006**, *125*, 049902, Publisher's note.

(59) Fernández-Ramos, A.; Ellingson, B. A.; Meana-Paneda, R.; Marques, J. M. C.; Truhlar, D. G. *Theor. Chem. Acc.* **2007**, *118*, 813.

(60) Hammond, G. S. *J. Am. Chem. Soc.* **1955**, *77*, 334.

(61) Karton, A.; Taylor, P. R.; Martin, J. M. L. *J. Chem. Phys.* **2007**, *127*, 064104.

(62) Bomble, Y. J.; Vázquez, J.; Kállay, M.; Michauk, C.; Szalay, P. G.; Császár, A. G.; Gauss, J.; Stanton, J. F. *J. Chem. Phys.* **2006**, *125*, 064108.

(63) Helgaker, T.; Klopper, W.; Koch, H.; Noga, J. *Chem. Phys.* **1997**, *106*, 9639.

(64) Luo, Y.-R. *Comprehensive Handbook of Chemical Bond Energies*; CRC Press: Boca Raton, 2007.

(65) Black, G. personal communication.

(66) Computational Chemistry Comparison and Benchmark DataBase http://srdata.nist.gov/cccbdb/.

JP8012464